Cell Reports, Volume *28*

Supplemental Information

Cryo-EM Studies of TMEM16F Calcium-Activated Ion Channel Suggest Features Important for Lipid Scrambling

Shengjie Feng, Shangyu Dang, Tina Wei Han, Wenlei Ye, Peng Jin, Tong Cheng, Junrui Li, Yuh Nung Jan, Lily Yeh Jan, and Yifan Cheng

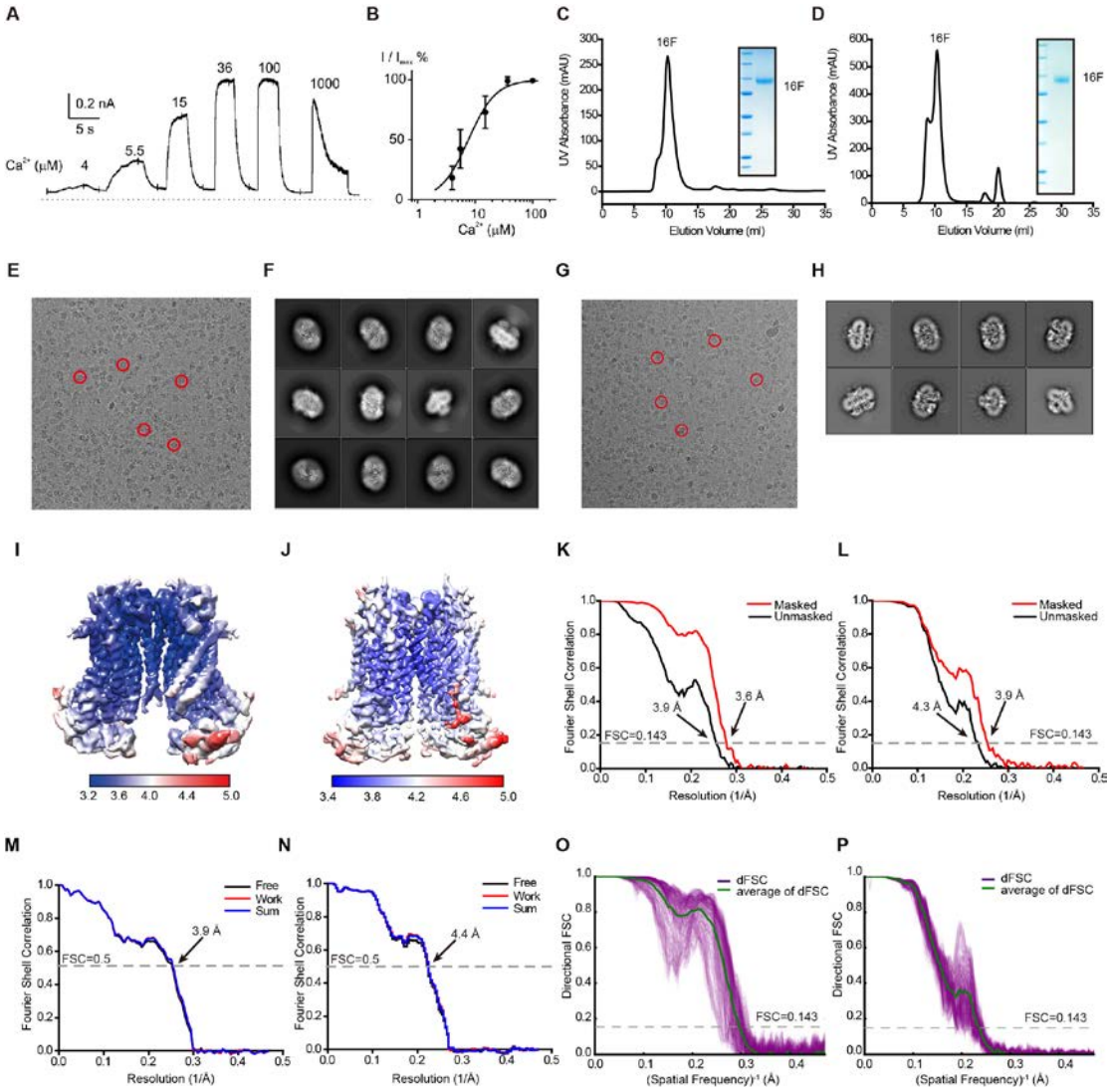

Figure S1. TMEM16F Protein Purification, Negative Staining, and Cryo-EM Analyses of TMEM16F in Digitonin. Related to Figure 1.

(A) Representative trace of inside-out patch from HEK293 cells transiently transfected with full-length TMEM16F. The membrane potential was held at 80 mV, and patches were exposed to increasing Ca^{2+} concentrations as indicated.

(B) Normalized currents were fit to the Hill equation (4 independent experiments, EC50 = 9.3 ± 3.0 μM, H = 1.8 ± 0.5).

(C, D) Size-exclusion chromatography of TMEM16F solubilized in digitonin with Ca^{2+} (C) or with EGTA (D). The peak fraction was examined by SDS-PAGE.

(E, G) Representative cryo-EM micrographs of Ca^{2+}-bound (E) and Ca^{2+}-free (G) TMEM16F in digitonin. Red circles indicate individual particles.

(F, H) Representative 2D-class averages of Ca^{2+}-bound (F) and Ca^{2+}-free (H) TMEM16F from boxed particles with 256-pixel box size (271.104 Å).

(I, J) Local resolution of Ca^{2+}-bound (I) and Ca^{2+}-free (J) TMEM16F, as estimated by RELION and shown with pseudo-color representation of resolution.

(K, L) FSC curves of two independently refined maps before (black) and after (red) post-processing in RELION of Ca^{2+}-bound (K) and Ca^{2+}-free (L) TMEM16F. Curves with resolution corresponding to

FSC = 0.143 are shown.

(M, N) FSC curves of free (black), work (red) and sum (blue) for processing of Ca^{2+}-bound (M) and Ca^{2+}-free (N) TMEM16F in digitonin. Curves with resolution corresponding to FSC = 0.5 are shown.

(O, P) dFSC from different Fourier cones for Ca^{2+}-bound (O) and Ca^{2+}-free (P) TMEM16F. Each curve indicates a different direction.

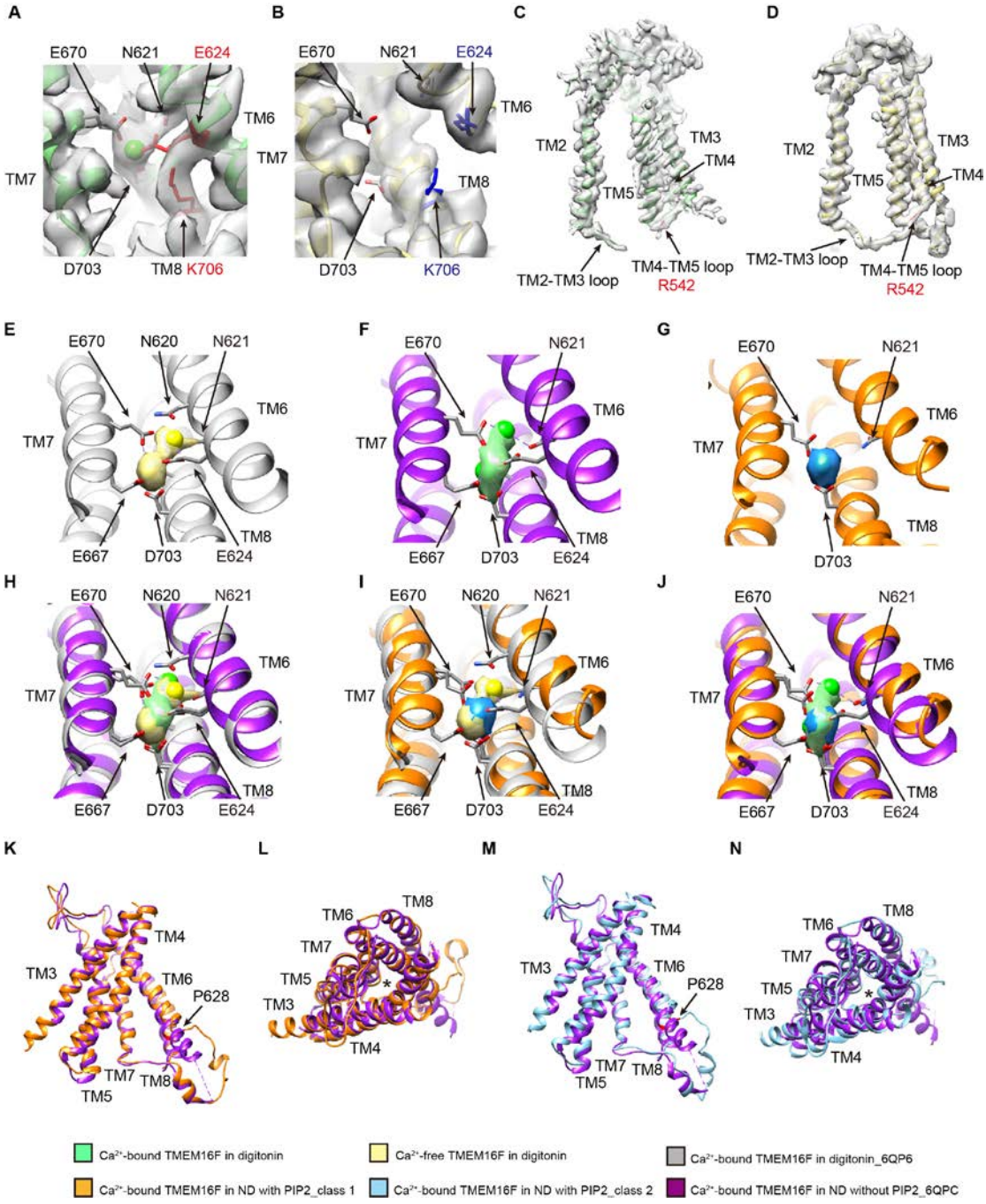

Figure S2. Ca^{2+} dependent conformation changes and comparison of TMEM16F structures with 6QP6 and 6QPC reported by Alvadia and colleagues. Related to Figures 1, 3 and 6.

(A-D) Ca^{2+} dependent conformation changes cause K706 to interact with E624 in Ca^{2+}-bound (A) but not Ca^{2+}-free (B) TMEM16F in digitonin. Likewise, R542 interacts with TM2-TM3 loop in Ca^{2+}-free (D) but not Ca^{2+}-bound (C) TMEM16F in digitonin.

(E-N) Pairwise superimposition of TM6-TM8 with Ca^{2+} coordinating residues (E-J) or pairwise superimposition of TM3-TM8 as pore-lining helices (K-N) in Ca^{2+}-bound TMEM16F in digitonin (green, from this study, or grey, for 6QP6), Ca^{2+}-free TMEM16F in digitonin (yellow), Ca^{2+}-bound TMEM16F in nanodiscs supplemented with PIP_2 (orange for class 1, blue for class 2), or Ca^{2+}-bound TMEM16F in nanodiscs without PIP_2 (purple, for 6QPC).

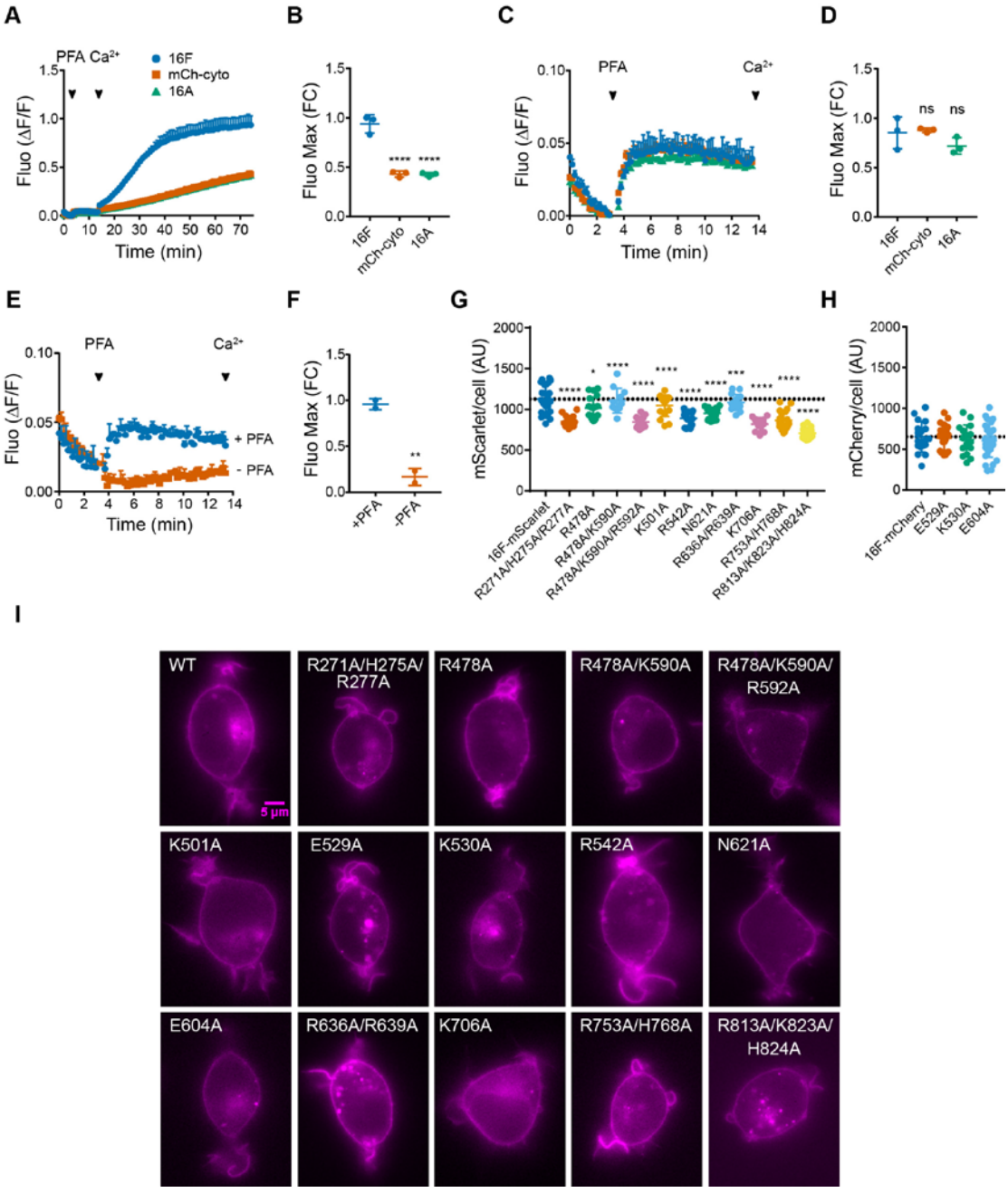

Figure S3. TMEM16F-dependent Ca^{2+} Influx in HEK293 Cells and Expression of TMEM16F Mutants with Alanine Substitutions. Related to Figures 2 and 4-6.

(A-F) Application of paraformaldehyde (PFA) for chemical induction of GPMV generation in Ca^{2+}-free extracellular solution followed with elevation of extracellular Ca^{2+} concentration to 2 mM ten minutes later revealed robust Ca^{2+} influx in cells expressing TMEM16F-mCherry but not control cells expressing TMEM16A-mCherry or soluble mCherry (mCh-cyto) (A, B). The Ca^{2+} rise in the absence

of extracellular Ca^{2+} does not require TMEM16F (C, D); this Ca^{2+} release from internal store is induced by the PFA treatment (E, F).

(G, H) Total protein expression of TMEM16F mutants tagged with mScarlet (G) or mCherry (H).

(I) Surface expression of TMEM16F tagged with mScarlet.

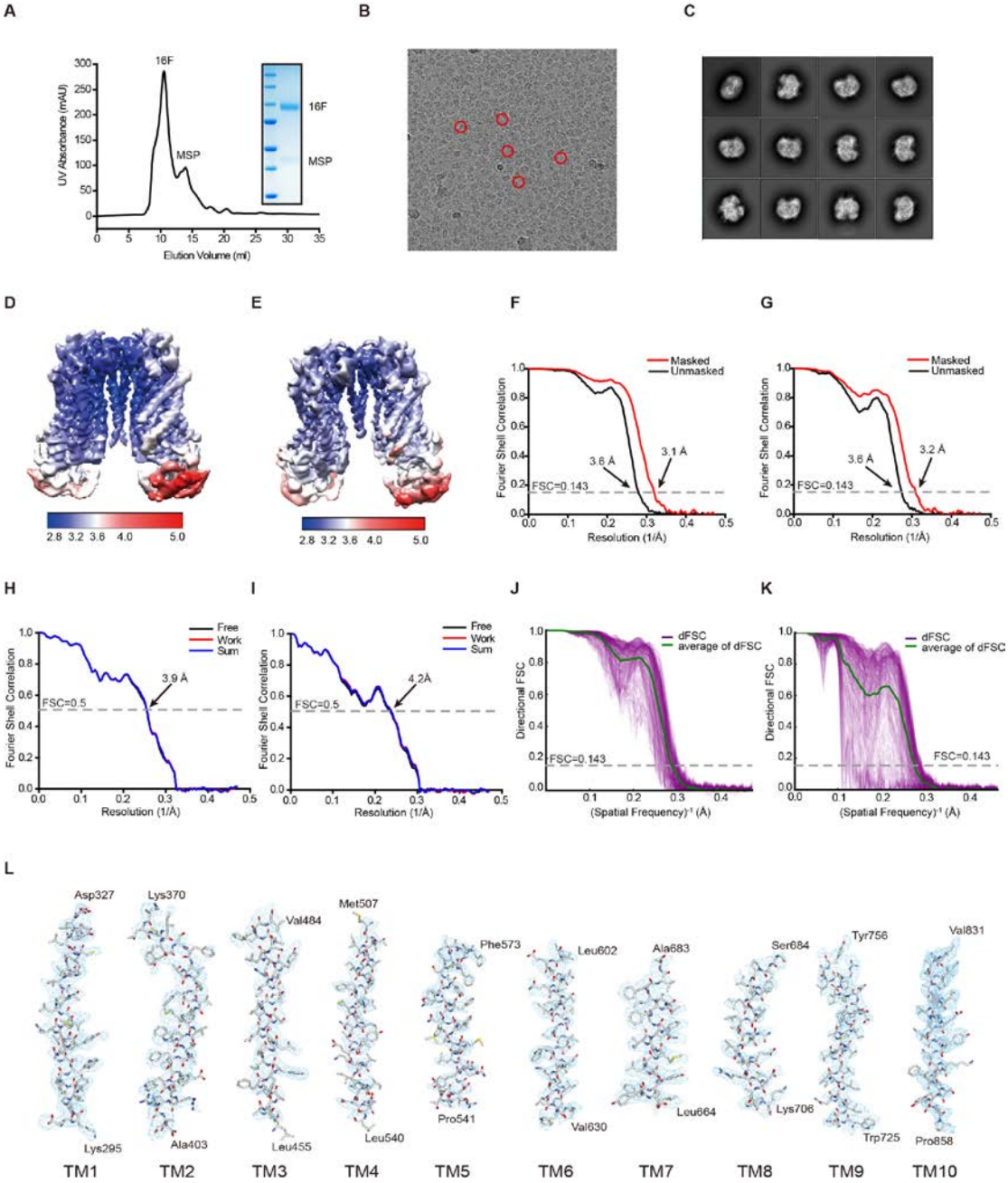

Figure S4. TMEM16F Protein Purification, Negative Staining, and Cryo-EM Analyses of TMEM16F in nanodiscs. Related to Figures 3-6.

(A) Size exclusion chromatography of TMEM16F reconstituted in lipid nanodiscs with MSP2N2. The peak fraction was examined by SDS-PAGE.

(B) Representative cryo-EM micrographs. Red circles indicate individual particles.

(C) Representative 2D-class averages from boxed particles with 256-pixel box size (271.104 Å).

(D, E) Local resolution of TMEM16F in PIP_2 supplemented nanodiscs (D for class 1, E for class 2), as

estimated by RELION and shown with pseudo-color representation of resolution.
(F, G) FSC curves of two independently refined maps before (black) and after (red) post-processing in RELION for TMEM16F in PIP_2 supplemented nanodiscs (F for class 1, G for class 2). Curves with resolution corresponding to FSC = 0.143 are shown.
(H, I) FSC curves of free (black), work (red) and sum (blue) for processing of Ca^{2+}-bound TMEM16F in PIP_2 supplemented nanodics (H for class 1, I for class 2). Curves with resolution corresponding to FSC = 0.5 are shown.
(J, K) dFSC from different Fourier cones for TMEM16F in PIP_2 supplemented nanodiscs (J for class 1, K for class 2). Each curve indicates a different direction.
(L) Representative cryo-EM densities of the ten transmembrane helices TM1-TM10 of TMEM16F (class 1) in PIP_2 supplemented nanodiscs. The electron microscopy densities are shown in blue and the model is shown as sticks colored according to atom type: C, light grey; N, blue; O, red; and S, yellow.

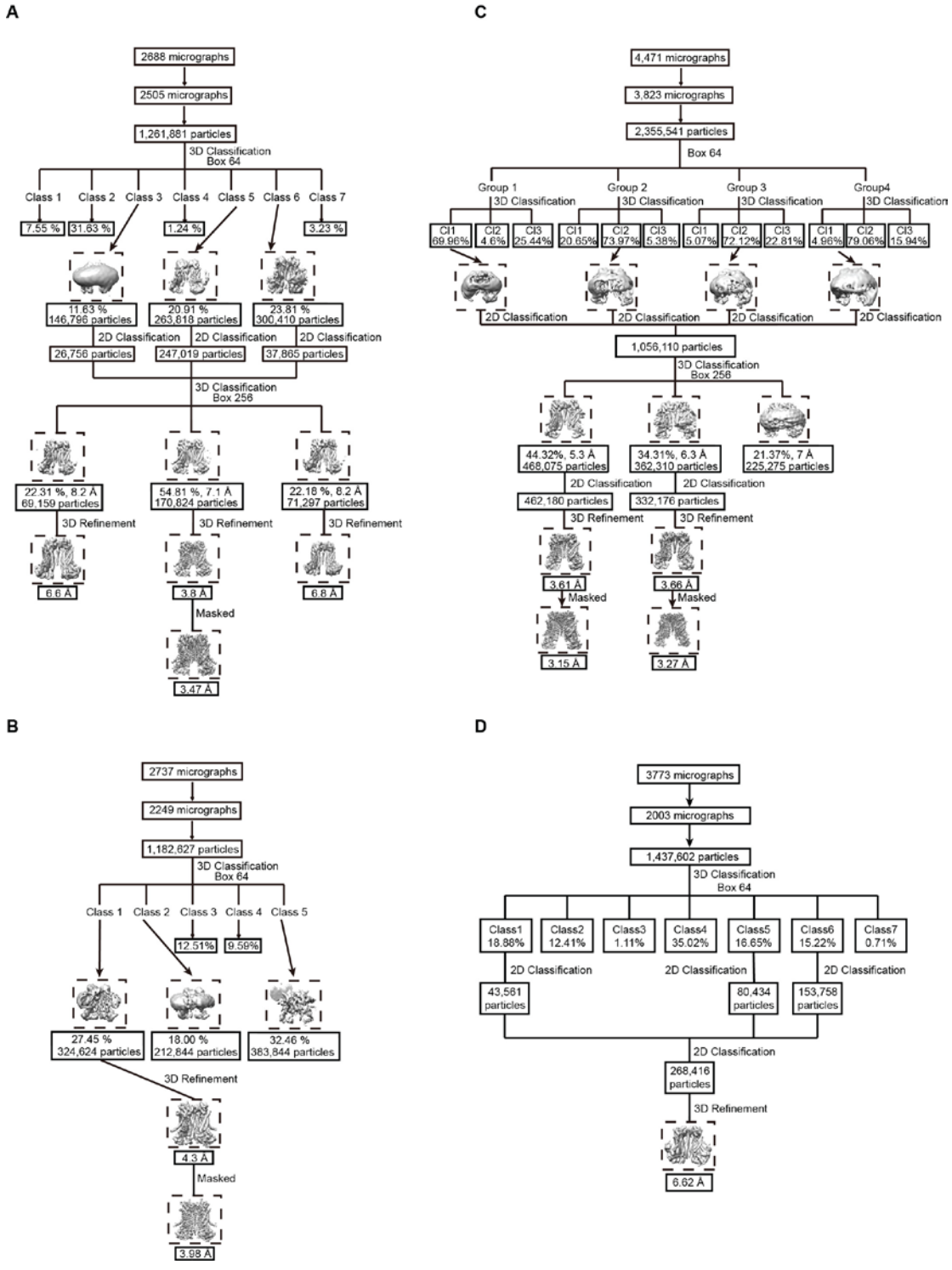

Figure S5. Cryo-EM Data Processing of TMEM16F. Related to Figures 1-7.

(A) Ca^{2+}-bound TMEM16F in digitonin. Starting with 3D classification of 1,261,881 particles, we picked class 3, 5, and 6 of the seven classes for 2D classification. After 2D classification was applied to each class, particles from the best 2D classes were pooled together for another round of 3D classification, to yield three classes for 3D refinement. The class with 170,824 particles had a resolution of 3.8 Å. After being masked, they reached a resolution of 3.7 Å.

(B) Ca^{2+}-free TMEM16F in digitonin. Starting with 3D classification of 1,182,627 particles, we picked class 1, 2, and 5 of the five classes for 2D classification. After 2D classification was applied to each

class, 324,624 particles from the best 2D classes were processed for another round of 3D classification and 3D refinement ending with a resolution of 4.3 Å. After being masked they reached a resolution of 3.98 Å.

(C) Ca^{2+}-bound TMEM16F in PIP_2 supplemented nanodiscs. All 2,355,541 picked particles were subdivided into four groups, and 3D classification was applied to each group to generate 3 classes. 2D classification was done for the best of the three classes of each group. Particles from the good 2D classes were pooled together (total 1,056,110 particles) and applied for another round of 3D classification to yield three classes. Class 1 and class 2 were picked for further 2D classification. Particles from the resulting good 2D classes were pooled together within each class and used for 3D refinement, resulting in a resolution of 3.61 Å for class 1 and 3.66 Å for class 2. After being masked, they reached a resolution of 3.15 Å for class 1 and 3.27 Å for class 2.

(D) Ca^{2+}-bound TMEM16F in nanodiscs without PIP_2 supplement. Starting with 3D classification of 1,437,602 particles, we picked class 1, 5 and 6 of the seven classes for 2D classification. After another round of 2D classification of these three classes combined, we picked 268,416 particles for 3D refinement ending with with a resolution of 6.62 Å.

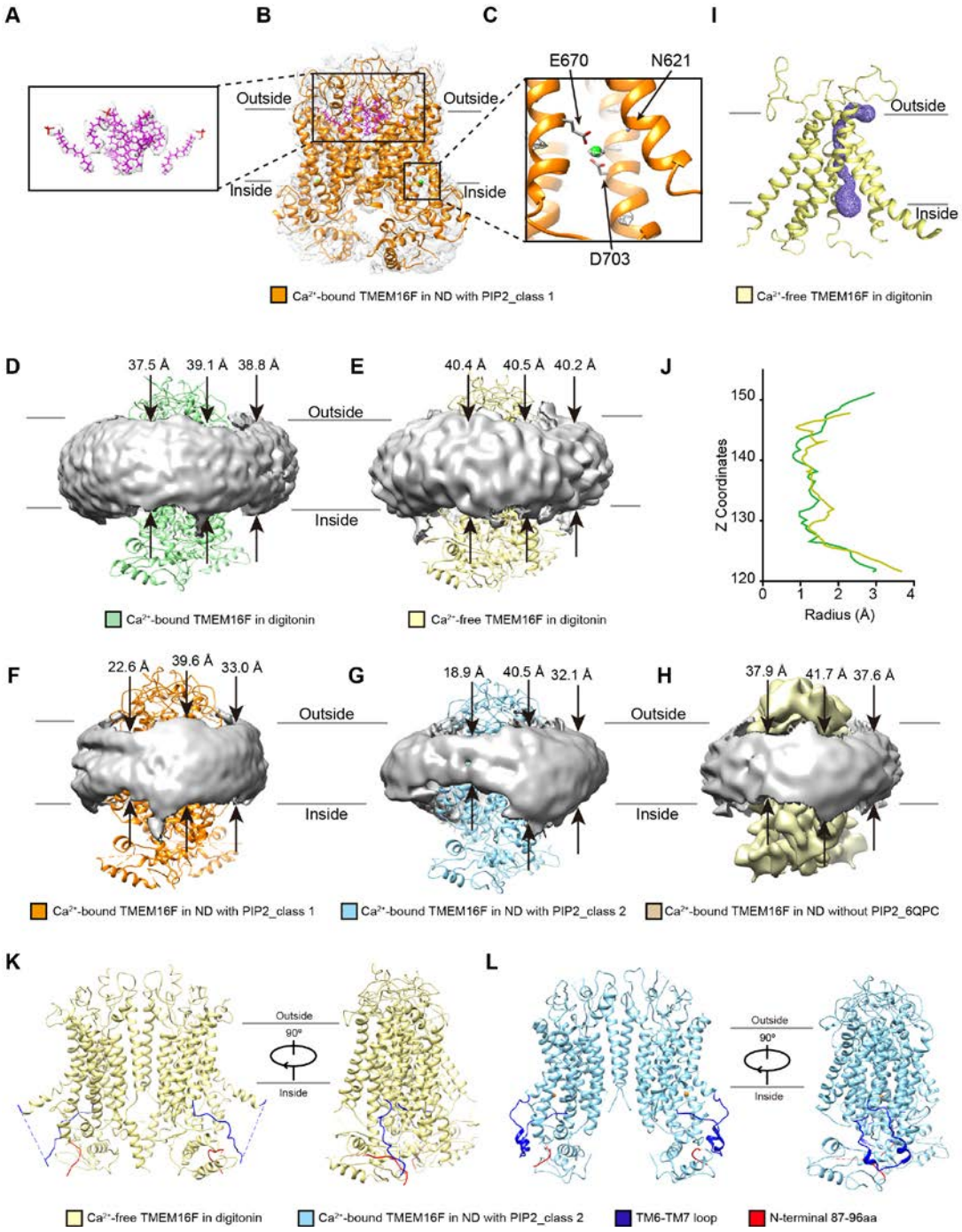

Figure S6. Ca^{2+}-free TMEM16F Channel Pore and Ca^{2+}-bound TMEM16F with PIP_2 Dependent Membrane Distortion. Related to Figures 3-6.

(A) Lipids with slanted orientations (model in magenta, superimposed on the sharpened electron density map in light grey) are associated with Ca^{2+}-bound TMEM16F in PIP_2 supplemented nanodiscs (class 1).

(B) Transmembrane helices and loops of TMEM16F in PIP_2 supplemented nanodiscs (class 1) (orange) with lipids (magenta) and one Ca^{2+} ion (green sphere) in each monomer, overlaid on the electron density map (sharpened, in light grey).

(C) One Ca^{2+} ion is coordinated by N621 on TM6, E670 on TM7 and D703 on TM8.

(D-H) Ca^{2+}-bound TMEM16F in digitonin (D), Ca^{2+}-free TMEM16F in digitonin (E), Ca^{2+}-bound

TMEM16F in nanodiscs without PIP_2 supplement (H), and Ca^{2+}-bound TMEM16F in PIP_2 supplemented nanodiscs (F, class 1; G, class 2). Measurements of the thickness of membranes in nanodiscs and micelle in digitonin solubilized TMEM16F reveal membrane distortion only for Ca^{2+}-bound TMEM16F in PIP_2 supplemented nanodiscs.

(I) The solvent-accessible (mesh) pore of Ca^{2+}-free TMEM16F in digitonin (yellow).

(J) Pore radius along the z axis for Ca^{2+}-free (yellow) and Ca^{2+}-bound (green) TMEM16F in digitonin.

(K, L) The basic residues in the N-terminal domain of TMEM16F that are crucial for PIP_2 modulation of channel activity are near the TM6-TM7 loop of Ca^{2+}-freeTMEM16F in digitonin (K) and Ca^{2+}-bound TMEM16F in nanodiscs supplemented with PIP_2 (L).

Figure S7. Sequence Alignment of Mouse and Human TMEM16F with Fungal Lipid Scramblase nhTMEM16 and Mouse TMEM16A. Related to Figure 7.

Residues in red boxes are identical in all four sequences, and those in orange boxes are highly conserved. TMEM16F residues in blue are tested in mutagenesis studies.

Table S1. Summary of Cryo-EM Data Collection and Model Refinement. Related to Figures 1 and 3-6.

	Digitonin_Ca	Digitonin	ND_Cl1	ND_Cl2
Data Collection/Processing				
Voltage (kV)	300	300	300	
Magnification	22,500	22,500	22,500	
Defocus Range (μm)	-0.5 – -2.7	-0.6 - -2.1	-0.5 – -2.9	
Pixel Size (Å)	1.059	1.059	1.059	
Total Electron Dose ($e^-/Å^2$)	48	72	56	
Exposure Time (s)	8	12	8	
Number of Images	2505	2249	3823	
Number of Frames/Image	40	120	40	
Initial Particle Number	1,261,881	1,182,627	2,355,541	
Final Particle Number	170,824	324,624	462,180	332,176
Resolution (unmasked, Å)	3.80	4.30	3.61	3.66
Resolution (masked, Å)	3.47	3.98	3.15	3.27
Refinement				
Number of Atoms	11,378	11,972	9,936	9,576
RMS Deviations				
Bond Lengths (Å)	0.006	0.005	0.011	0.006
Bond Angles (^{o})	1.020	1.038	1.259	1.140
Ramachandran				
Favored (%)	97.32	96.04	97.60	94.87
Allowed (%)	2.53	3.68	1.88	4.42
Outlier (%)	0.15	0.28	0.52	0.71
Molprobity Score	2.04	2.43	2.14	2.29
EMRinger Score	1.68	1.66	1.48	0.96

Table S2. Structure-based Mutagenesis. Related to Figures 2 and 4-6.

Time of onset, V_{max} and Max values of Ca^{2+} rise, PS exposure, and GPMV generation of wildtype (WT) and mutant TMEM16F. Time-lapse imaging of 500-1000 cells with 10X magnification was performed to concurrently monitor GPMV formation and Ca^{2+} influx via Fluo-8 fluorescence. Time-lapse imaging of individual cells viewed with 60X magnification was performed to monitor PS exposure via pSIVA fluorescence. Time of onset could not be determined for those time courses of TMEM16F-dependent Ca^{2+} rise that are linear rather than sigmoidal, nor could Vmax and time of onset be determined for those cases with minimal PS exposure and/or GPMV generation. All measurements are normalized by expression levels. * $p < 0.05$, ** $p < 0.01$, *** $p < 0.001$, **** $p < 0.0001$. Statistical significance of all mutants as compared to TMEM16F wildtype (WT) are determined by one-way ANOVA followed by Holm- Šídák multiple comparisons test.

Mutation	WT	R271A/H275A/R277A	R478A	R478A/K590A	R478A/K590A/R592A	E529A	K530A	R542A	E604A	N621A	R636A/R639A	K706A	R753A/H768A	R813A/K823A/H824A
Position	16F	pre-TM1 elbow	TM3	TM3/TM5-TM6 loop	TM3/TM5-TM6 loop	TM4	TM4	TM4-TM5 loop	TM6	TM6	TM6	TM8	TM9-TM10 loop	TM9-TM10 loop
Fluo Max														
N	14	6	6	6	6	3	3	5	2	6	6	6	6	6
					(linear)					(linear)		(linear)		(linear)
Mean	0.66615	0.704339085	0.71151	0.598756243	0.527117203	0.96826	1.05811	0.616758582	0.45905	0.37009	0.541198612	0.42424	0.449273874	0.462253634
stdev	0.11337	0.158630761	0.13779	0.036537966	0.090324578	0.0112	0.06877	0.045863595	0.07584	0.03393	0.212836465	0.06655	0.025013127	0.054106781
SEM	0.0303	0.064760737	0.05625	0.014916562	0.036874855	0.00646	0.0397	0.020510823	0.04379	0.01385	0.086890123	0.02717	0.010211567	0.022089001
p-value		0.9894	0.9662	0.7602	0.0715	0.5632	0.0609	0.9619	0.0004	**<0.0001**	0.1313	**0.0002**	**0.001**	**0.0022**
Fluo Vmax														
N	13	6	6	6	6	3	3	5		6	6	6	6	6
					(linear)				N/A	(linear)		(linear)		(linear)
Mean	0.02513	0.081393	0.02029	0.014951	0.007356167	0.04238	0.0344	0.012323333		0.00804	0.031512667	0.00506	0.014037	0.005519333
stdev	0.0047	0.026974725	0.00361	0.001601364	0.001267939	0.00023	0.00136	0.001204038		0.00092	0.011590094	0.00072	0.001084139	0.000435437
SEM	0.0013	0.011012385	0.00147	0.000653754	0.000517634	0.00013	0.00079	0.000491547		0.00038	0.004731636	0.00029	0.000442598	0.000177766
p-value		**<0.0001**	**0.0015**	**<0.0001**	**<0.0001**	**0.0006**	0.0501	**<0.0001**		**<0.0001**	0.2876	**<0.0001**	0.1343	**0.0068**
Fluo Onset														
N	13	6	6	6		3	3	5			6		6	
					N/A				N/A	N/A		N/A		N/A
Mean	23.2	17.56666667	25.9333	23		29.6	15.9333	11.9			22.46666667		23.96666667	
stdev	1.87794	0.480277697	1.05578	0.45607017		0.34641	1.51438	6.448255578			0.43204938		0.763326055	
SEM	0.52085	0.196072549	0.43102	0.186189867		0.2	0.87433	2.632489316			0.176383421		0.311626557	
p-value		**<0.0001**	0.1614	0.9805		**<0.0001**	**0.0046**	<0.0001			0.4388		0.4388	
pSIVA Max														
N	25	16	19	11	14	13	9	18	15	17	14	11	19	15
Mean	0.9937	0.771636318	0.80995	0.586273909	0.398015286	0.53127	0.87081	0.958964611	0.52172	0.28223	0.8811155	0.8148	0.647502526	0.6920274
stdev	0.18729	0.103622183	0.09234	0.096780798	0.246367709	0.19486	0.2048	0.231983264	0.16971	0.09373	0.098881636	0.22995	0.2114395	0.156726146
SEM	0.03746	0.025905546	0.02118	0.029180509	0.06584454	0.05404	0.06827	0.05467898	0.04382	0.02273	0.026427229	0.06933	0.048507548	0.040466517
p-value		**0.0001**	**0.002**	**<0.0001**	**<0.0001**	0.182	0.0736	0.5012	0.182	**<0.0001**	**0.0437**	**0.0127**	**<0.0001**	**<0.0001**
pSIVA Vmax														
N	25	16	19	11	12	13	9	13	15	17	14	11	19	15
Mean	0.05711	0.038996563	0.04587	0.025084636	0.021032167	0.02082	0.0336	0.079541538	0.01635	0.0108	0.054629214	0.03579	0.043395158	0.0420674
stdev	0.02362	0.010578762	0.00903	0.004990293	0.011223954	0.00888	0.00784	0.018021241	0.00493	0.00363	0.023248434	0.01388	0.016571411	0.013137322
SEM	0.00472	0.002644691	0.00207	0.00150463	0.003240076	0.00246	0.00261	0.004998193	0.00127	0.00088	0.006213405	0.00418	0.003801743	0.003392042
p-value		**0.0133**	**0.034**	**<0.0001**	**<0.0001**	0.3398	**0.0311**	**<0.0001**	0.0536	**<0.0001**	0.6926	**0.0004**	**0.0471**	**0.0471**
pSIVA Onset														
N	25	16	19	11	12	13	9	13	15	17	14	11	19	15
Mean	23.2	17.45	25.6842	30.18181818	37.9	30.5538	22.2444	6.446153846	25.4667	33.5294	16.75714286	24.6909	45.42105263	36.65333333
stdev	4.36348	5.799540212	7.74147	8.0956554	9.496602263	7.53753	6.95326	1.741941151	7.33121	4.60866	4.279596366	5.1376	6.656957843	7.330354373
SEM	0.8727	1.449885053	1.77601	2.440931945	2.741432937	2.09053	2.31775	0.483127549	1.89291	1.11776	1.14377024	1.54904	1.527210869	1.892689361
p-value		**0.0023**	0.5848	0.0517	**<0.0001**	**0.0006**	0.2665	**<0.0001**	**0.0376**	**<0.0001**	**0.0022**	0.7663	**<0.0001**	**<0.0001**
GPMV Total														
N	14	6	6	6	6	6	6	6	6	6	6	6	6	6
Mean	0.80494	2.028787547	0.7418	0.166234468	0.031667143	0.69605	1.87103	0.992064731	0.01073	0.01398	0.474024579	0.08615	0.414088884	0.177070437
stdev	0.18721	0.642700124	0.14534	0.03834898	0.039727935	0.07407	0.11065	0.064976373	0.00777	0.01843	0.289026413	0.0166	0.079901225	0.032799919
SEM	0.05003	0.262381227	0.05933	0.015655905	0.016218861	0.03024	0.04517	0.029058317	0.00317	0.00752	0.117994539	0.00678	0.032619538	0.013390511
p-value		**<0.0001**	0.9966	**<0.0001**	**<0.0001**	**<0.0001**	0.8818	**0.5283**	**<0.0001**	**<0.0001**	**0.0279**	**<0.0001**	**0.0059**	**<0.0001**
GPMV Vmax														
N	13	6	6	6		6	6	6			6	6	6	6
					N/A				N/A	N/A				
Mean	0.04367	0.081393	0.04599	0.013307167		0.0504	0.09119	0.036998			0.0254235	0.00549	0.019469167	0.008437333
stdev	0.00757	0.026974725	0.01102	0.003585832		0.00604	0.00931	0.004099936			0.014510598	0.00125	0.003540685	0.002859481
SEM	0.0021	0.011012385	0.0045	0.00146391		0.00247	0.0038	0.001673792			0.005923927	0.00051	0.001445479	0.001167378
p-value		**<0.0001**	0.5512	**<0.0001**		**<0.0001**	0.6936	0.1188			**0.0081**	**<0.0001**	**0.0014**	**<0.0001**
GPMV Onset														
N	13	6	6	6		6	6	6			6	6	6	6
					N/A				N/A	N/A				
Mean	32.6923	20.23333333	40.6	44.6		43.4333	19.1667	26.2			27.23333333	45.8	33.1	43.5
stdev	3.68837	0.637704216	1.26491	0.971596624		0.95009	0.88015	1.152388823			0.907009739	1.86333	0.81731267	3.384080377
SEM	1.02297	0.260341656	0.5164	0.396652661		0.38787	0.35932	0.470460767			0.370285175	0.7607	0.3336665	1.381545029
p-value		**<0.0001**	**<0.0001**	**<0.0001**		**<0.0001**	**0.0009**	**<0.0001**			**0.0005**	**<0.0001**	0.76	**<0.0001**